

Fractal two-dimensional electromagnetic band-gap structures

F. Frezza*, L. Pajewski*, and G. Schettini**,

*Department of Electronic Engineering, "La Sapienza" University of Rome, Via Eudossiana 18, 00184 Roma, Italy.

**Department of Applied Electronics, "Roma Tre" University of Rome, Via della Vasca Navale 84, 00146 Roma, Italy.

Abstract—Fractal two-dimensional Electromagnetic Band-Gap (EBG) materials are proposed and studied by means of a full-wave method developed for diffraction gratings. Such technique allows us to characterize, in a rapidly convergent way, the transmission and reflection properties of periodic fractal structures with an arbitrary geometry in the unit cell. Both polarization cases can be treated. In particular, two different fractal EBG materials are considered. Numerical results are reported for the transmission efficiency as a function of the frequency. Typical effects due to the fractal geometry are observed, like multi-band behavior and enlargement of stop-bands.

I. INTRODUCTION

As is well known, Electromagnetic Band-Gap (EBG) materials are periodic structures that exhibit frequency bands within which the waves are highly attenuated and the propagation is prohibited [1]. This property has been exploited in a lot of applications at optical, millimeter-wave and microwave frequencies: EBG waveguides [2], resonators [3], microstrip structures [4], and more, have been proposed.

Most EBG applications deal with two-dimensional (2D) materials, invariant along a longitudinal axis and periodic in the transverse plane [5], since they are easier to manufacture and they can show strong angular reflectivity properties over a wide frequency band. In 2D-EBG materials, rods of a specific permittivity are embedded in a homogeneous background of different permittivity.

To obtain stopbands as large as possible is a fundamental target in EBG design: to this aim simple geometries with different rod section shapes have been investigated [6], and optimization techniques have been applied to suitably shape the cross-section of the rods [7].

In some applications a multiband frequency response of the EBG material is required: in fact, even if an EBG structure presenting a wide stop-band is used, it may happen that the required stop-bands are not all within this spectrum. In order to realize an EBG structure which shows multiband and wide stop-band properties, it is natural to make use of fractals.

Fractals were first defined by Mandelbrot [8] as shapes made of parts similar to the whole in some way. A wide variety of applications have been found for fractals in many branches of science and engineering [9]. In the area of fractal electrodynamics, the electromagnetic-wave interactions with fractal objects are investigated, and a new class of radiation, propagation, and scattering problems are treated [10].

The self-similarity property of fractal shapes, i.e. the

replication of the geometry at different scales within the same structure, results in a multiband behavior making fractals specially suitable to design multifrequency antennas [10], [11] and antenna arrays [10], [12]. The same property has been exploited also in the design of multiband frequency selective surfaces [13].

Fractal geometries have been employed in a quite simple PBG microstrip structure where microstrip lines with few etched fractal holes in the ground plane have been studied and measured [14], showing dual-stopband characteristics.

In this paper, we propose novel EBG materials made of dielectric rods with fractal cross-sections. Due to the fractal self-similarity of the rods, multiband frequency responses and wider stop-bands are observed, if compared with those of EBG materials made of rods with simple geometrical shapes. To our knowledge, it is the first time that the characteristics of fractal 2D-EBG dielectric materials are investigated. The results of this work show that the application of fractal geometries in EBG design is a promising area of research.

In Section II, we briefly summarize the formulation of the full-wave theory employed by us to model and characterize 2D-EBG materials [16]. In Section III we describe the novel fractal EBG structures that we considered. In Section IV, we present numerical results showing the frequency responses of the proposed structures. In Section V, we give the conclusions.

II. CHARACTERIZATION OF 2D-EBG STRUCTURES THROUGH A FULL-WAVE METHOD FOR GRATINGS

The formulation of our theory can be found in [15], [16]. We showed that an accurate and efficient characterization of 2D-EBG structures can be performed exploiting a full-wave diffraction theory developed for one-dimensional diffraction gratings. In fact, a 2D electromagnetic crystal may be considered as a stack of periodic grids of rods separated by homogeneous layers, i.e. as a stack of one-dimensional diffraction gratings.

Our method applies both to TE (electric field parallel to the grating grooves) and TM (magnetic field parallel to the grating grooves) polarizations. Briefly, we consider a monochromatic plane wave of wavelength λ (in a vacuum), impinging at an angle θ on a multilevel dielectric grating. The typical layer of the multilevel structure is a binary grating including several alternate regions of different refractive indices. The multilevel grating is bounded by



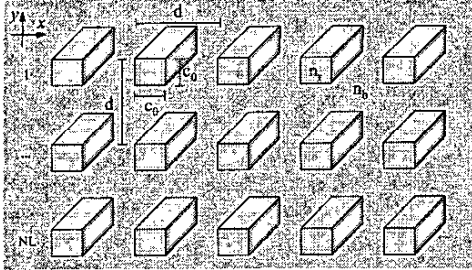


Fig. 1. A square-lattice EBG material of square-section rods.

two possibly different media. The general approach for exactly solving the electromagnetic problem associated with the diffraction grating involves the solution of Maxwell's equations in the incidence region, the grating layers, and the transmission region. By applying the boundary conditions between different layers, a resulting equation system is found. In order to solve this system and, as a consequence, to compute the reflected and transmitted field amplitudes, and the diffraction efficiencies, appropriate techniques must be employed. Care has to be used to overcome numerical problems due to ill-conditioned matrices obtained on imposing the boundary conditions, and to improve numerical stability and efficiency of the implemented codes.

With this method it is possible to study EBG materials made of rods or holes in a host medium, with arbitrary shape and forming whatever kind of lattice. The involved materials can be isotropic or anisotropic dielectrics or metals, and losses can be taken into account. The structures have a finite thickness, i.e. they infinitely extend only in two dimensions.

III. FRACTAL 2D-EBG STRUCTURES

A square-lattice EBG material is sketched in Fig. 1: the period of the structure is chosen to be the same along x and y , and it is called d ; n_r and n_b are the refractive indices of rod and background media, respectively. We denote with NL the number of rod layers, along y . The unit cells of the novel fractal 2D-EBG structures proposed in this work are given in Figs. 2 and 3: the generator is always a square rod section of side length c_0 , as in Fig. 1.

For what concerns the unit-cell-generation of the first structure (Fig. 2), at each iteration a square is added to the middle of every side of the rod section: the side of the added square is one third of the side close to which it is placed. The rod section obtained after one iteration is reported in Fig. 2(a), where $c_1 = c_0/3$; after two iterations the rod section of Fig. 2(b) is generated, where $c_2 = c_1/3$.

The second structure (Fig. 3) is generated subtracting, at each iteration, a square to each side of the rod section: the side of the subtracted square is one fourth of the side from which it is cut. After one and two iterations, the rod sections that we obtained are reported in Figs. 3(a) and 3(b), respectively.

For each geometrical configuration, it is customary to

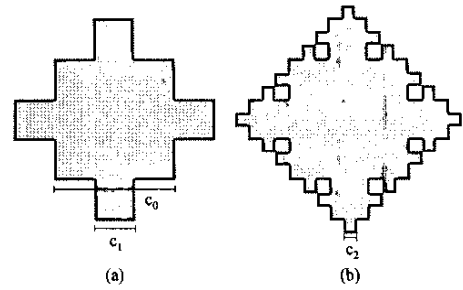


Fig. 2. (a) One iteration (b) Two iterations

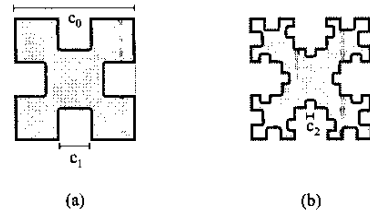


Fig. 3. (a) One iteration (b) Two iterations

define the so-called filling factor F , which represents the fraction of the unit cell of the periodic structure filled by the rod. At iteration 0, we have $F = c_0^2$. After one iteration the filling factor is $F = 13c_1^2$, $20c_1^2$, and $12c_1^2$, and after two iterations it is $F = 137c_2^2$, $350c_2^2$, and $162c_2^2$, for the first, the second and the third structure, respectively. The filling factor is a parameter that greatly affects the transmission and reflection properties of an EBG material. Since our interest is in understanding the effects of the fractal cross-section and in comparing it with standard geometries, in our simulations we have rescaled all the structures to have the same filling factor.

We denote with η_T the total transmission efficiency of the EBG structure, that is, the sum of the efficiencies of all the transmitted orders (the efficiency of the n -th transmitted order is the ratio between the Poynting-vector y -component of the n -th order transmitted wave and that of the incident wave). Analogously, we denote with η_R the total reflection efficiency.

Unless otherwise specified, the incident plane wave is supposed to impinge normally on the structure.

IV. NUMERICAL RESULTS

Let us consider an EBG structure made of a stack of $NL = 20$ layers, with rods having the fractal cross-section shown in Fig. 2. The filling factor is $F = 0.25$. The rod refractive index is $n_r = 2$ and the host medium is supposed to be a vacuum ($n_b = 1$). First of all, we checked the convergence properties of our rigorous method when applied to this kind of EBG material: we have a very good convergence rate in both polarization cases, but the relevant results are not shown here for brevity.

In Fig. 4, the transmission efficiency η_T (solid line) is

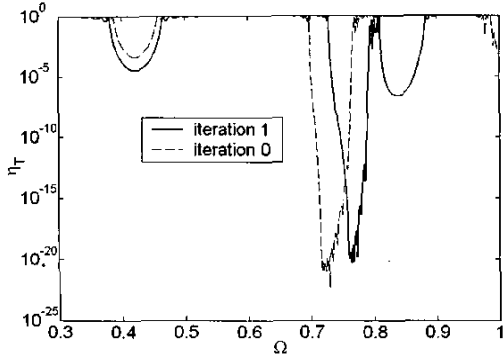


Fig. 4. Transmission efficiency η_T (solid line), as a function of the normalized frequency Ω , for the EBG structure of Fig. 2(a). The polarization is TM. The behavior of the structure made of square-section rods (iteration 0, dashed line) is also shown, for comparison.

shown, in a logarithmic scale, as a function of the normalized frequency $\Omega = \frac{\omega d}{2\pi c}$ (c being the light velocity in a vacuum and ω being the angular frequency), for the EBG structure obtained after one iteration. The polarization is TM and the behavior of the material made of square-section rods (iteration 0, dashed line) is also shown; for comparison. It can be noted that, when the details of the structure are small with respect to the incident wavelength, the use of a fractal rod section has not a great effect on the frequency stop-bands of the structure: as Ω decreases, due to an averaging phenomenon, the behavior of the EBG material (for a given polarization and incidence angle) depends only on the filling factor and on the refractive index of the rod material, while the rod shape becomes less and less important. However, the gap centered on $\Omega_c \cong 0.42$ is slightly wider and deeper for the fractal EBG material: we have $\eta_T \leq 0.01$ when $0.396 < \Omega < 0.436$ and when $0.393 < \Omega < 0.452$, for the 0-iteration and 1-iteration structures, respectively; moreover, $\eta_T \cong 3 \cdot 10^{-4}$ and $\eta_T \cong 2 \cdot 10^{-5}$ for the 0-iteration and 1-iteration structures, respectively, in the deepest point of the stop-band. The fractal rod section has a more interesting effect on the stop-bands of the EBG material for higher values of the normalized frequency Ω : in fact, it can be noted that the 0-iteration stop-band centered on $\Omega_c \cong 0.73$ shifts toward higher values of Ω (in particular, it is centered on $\Omega_c \cong 0.76$ for the 1-iteration structure); moreover, a new stop-band is present, centered on $\Omega_c \cong 0.845$. Such multi-band behavior is typical of fractal geometries. The responses of the 1-iteration and 2-iteration structures are very similar in this frequency range, except for negligible differences in central frequencies and depths of the stop-bands, therefore the curve for the 2-iteration structure is not reported here.

For what concerns TE polarization, in the $\Omega \leq 1$ range the use of fractal-section rods has not a significant effect on the frequency stop-bands of the structure, and so the relevant curves are not reported here. However, in Fig. 5 η_T is shown as a function of the normalized frequency Ω for the 2-iteration (solid black line), 1-iteration (solid gray line) and 0-iteration (dashed line) structures, when $1.5 \leq \Omega \leq 2$. It can be seen that for the structure made of square-section

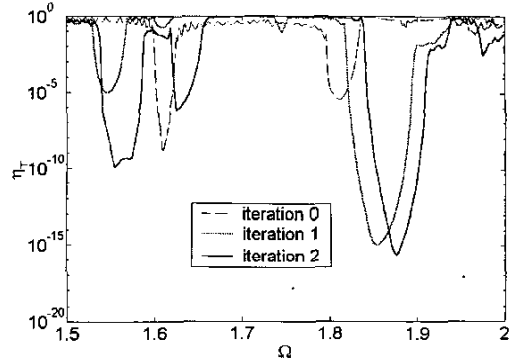


Fig. 5. Transmission efficiency η_T (solid line), as a function of the normalized frequency Ω , for the EBG structure of Fig. 2. The polarization is TE. The behavior of the structure made of square-section rods (iteration 0, dashed line) is also shown, for comparison.

rods there are only two small stop-bands in this range, centered on $\Omega_c \cong 1.61$ and 1.81 , and of width $\Delta\Omega \cong 0.025$ and 0.036 ($\eta_T \leq 0.01$), respectively. For the 1-iteration structure, the first stop-band shifts toward smaller values of Ω and becomes about two times larger but less deep: it is centered on $\Omega_c \cong 1.54$ and $\Delta\Omega \cong 0.052$ wide; the second stop-band, instead, shifts toward higher values of Ω and becomes much wider and deeper: it is centered on $\Omega_c \cong 1.86$, $\Delta\Omega \cong 0.081$ wide, and in the deepest point η_T reaches 10^{-15} . The last mentioned stop-band is of particular interest for high-frequency applications: for two different EBG materials possessing stop-bands of equal size, it may be advantageous from a fabrication standpoint to choose the one that has the stop-band occurring at the higher normalized frequency Ω , since the feature size scales with d . For the 2-iteration structure, the first stop-band splits into two wider stop-bands: they are centered on $\Omega_c \cong 1.56$ and 1.64 , and their widths are $\Delta\Omega \cong 0.050$ and 0.032 , respectively; the one centered on $\Omega_c \cong 1.56$ is very deep, in fact η_T reaches 10^{-10} . Also for the 2-iteration structure there is a wide, deep stop-band at higher values of Ω , very similar to the one obtained for the 1-iteration structure: it is centered on $\Omega_c \cong 1.88$, $\Delta\Omega \cong 0.081$ wide, and in the deepest point η_T reaches $2 \cdot 10^{-16}$. In conclusion, it can be seen that the fractal geometry can not only create new stop-bands but also enlarge the existing ones.

Let us now consider an EBG structure made of a stack of $NL = 20$ layers, with rods having the fractal cross-section shown in Fig. 3. The filling factor is also in this case $F = 0.25$, the rod refractive index is $n_r = 2$ and the host medium is supposed to be a vacuum ($n_b = 1$). We checked the convergence properties of our method when applied to this kind of EBG material, with very good results.

In Fig. 6, the transmission efficiency η_T (solid line) is shown as a function of the normalized frequency Ω , for the EBG structure obtained after two iterations (Fig. 3(b)). Both polarization cases are reported in the figure, and the behavior of the material made of square-section rods (iteration 0, TM pol.: dashed line, TE pol.: dotted line) is also shown, for comparison. For what concerns TM polarization, the 0-iteration stop-band centered on $\Omega_c \cong 0.42$

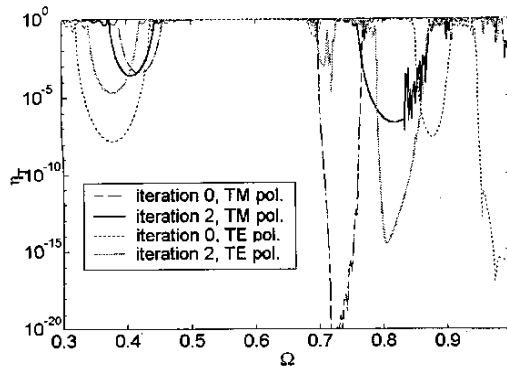


Fig. 6. Transmission efficiency η_T (solid line), as a function of the normalized frequency Ω , for the EBG structure of Fig. 3(b). The behavior of the structure made of square-section rods (iteration 0, dashed and dotted lines) is also shown, for comparison. Both polarization cases are reported in the figure.

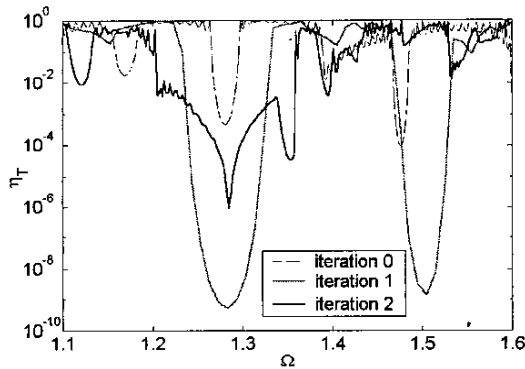


Fig. 7. Transmission efficiency η_T (solid line), as a function of the normalized frequency Ω , for the EBG structure of Fig. 3. The polarization is TE. The behavior of the structure made of square-section rods (iteration 0, dashed line) is also shown, for comparison.

shifts toward slightly smaller values of Ω for the 2-iteration structure; it is interesting to note that the 0-iteration stop-band centered on $\Omega_c \cong 0.73$ shifts toward higher values of Ω and appreciably changes its shape, becoming less deep but much wider (it is $\Delta\Omega \cong 0.11$ wide). For what concerns TE polarization, it can be seen that the 0-iteration stop-band centered on $\Omega_c \cong 0.88$ shifts toward smaller values of Ω , becoming centered on $\Omega_c \cong 0.83$ and $\Delta\Omega \cong 0.077$ wide: such shift is important since it causes the overlapping of TM and TE stop-bands, and therefore the formation of a wide complete stop-band which is absent in the non-fractal structure. In fact, we recall that a complete 2D stopband occurs if the stop-bands for both polarization cases are present and they overlap each other.

In Fig. 7, η_T is shown as a function of Ω , for the 2-iteration (solid black line), 1-iteration (solid gray line) and 0-iteration (dashed line) structures, when $1.1 \leq \Omega \leq 1.6$. The polarization is TE. For what concerns the 1-iteration structure, it is interesting to note the presence of two wide and deep stop-bands: they are centered on $\Omega_c \cong 1.28$ and 1.5, and they are $\Delta\Omega \cong 0.093$ and 0.060 wide, respectively. As far as the 2-iteration structure is concerned, the existing stop-band centered on $\Omega_c \cong 1.2815$ greatly enlarges,

becoming $\Delta\Omega \cong 0.153$ wide.

V. CONCLUSION

In this work the transmission properties of a class of fractal periodic structures have been studied by means of a numerical technique originally developed for diffraction gratings. Two examples of fractal EBG materials have been proposed and analyzed. The obtained results are very promising, showing that the fractal geometry produces the expected effects, like the appearance of new stop-bands (also of the complete type) and the enlargement of the existing ones. Such properties could be exploited in many applications where a multi-band frequency behavior is required, or wider stop-bands are needed. The employed approach is indeed very general and can deal with arbitrary fractal geometries of the unit-cell.

REFERENCES

- [1] J. D. Joannopoulos, R. D. Meade, and J. N. Winn, *Photonic Crystals: Molding the Flow of Light*, Princeton University Press, Princeton, NJ, 1995.
- [2] J. G. Maloney, M. P. Kesler, B. L. Shirley, and G. S. Smith, "A simple description for waveguiding in photonic bandgap materials," *Microwave and Opt. Technol. Lett.*, vol. 14, pp. 261-266, Apr. 1997.
- [3] H. Contopanagos, N. G. Alexopoulos, and E. Yablonovitch, "High Q radio frequency structures using one-dimensionally periodic metallic films," *IEEE Trans. Microwave Theory Tech.*, vol. 46, pp. 1310-1312, Sept. 1998.
- [4] H. Contopanagos, N. G. Alexopoulos, and E. Yablonovitch, "Photonic band-gap materials as all-dielectric planar reflectors," *Microwave and Opt. Technol. Lett.*, vol. 11, 169-174, Mar. 1996.
- [5] T. Lopetegi, M. A. G. Laso, R. Gonzalo, M. J. Erro, F. Falcone, D. Benito, M. J. Goude, P. De Maagt, and M. Sorolla, "Electromagnetic crystals in microstrip technology," *Opt. and Quantum Electronics*, vol. 34, pp. 279-295, Jan.-Mar. 2002.
- [6] H. Y. D. Yang, "Finite Difference Analysis of 2-D Photonic Crystals," *IEEE Trans. Microwave Theory Tech.*, vol. 44, pp. 2688-2695, Dec. 1996.
- [7] S. T. Peng and R. B. Hwang, "Dispersion characteristics of two-dimensionally periodic structures," *Proc. 2001 URSI International Symposium on Electromagnetic Theory*, pp. 317-319, Victoria, Canada, May 2001.
- [8] M. Qiu and S. He, "Optimal design of a two-dimensional photonic crystal of square lattice with a large complete two-dimensional bandgap," *J. Opt. Soc. Am. B*, vol. 17, pp. 1027-1030, Jun. 2000.
- [9] B. B. Mandelbrot, *The fractal geometry of nature*, W. H. Freeman, New York, 1983.
- [10] J. L. Vehel, E. Lutton, and C. Tricot, eds., *Fractals in engineering*, Springer-Verlag, New York, 1997.
- [11] D. H. Werner and R. Mittra, eds., *Frontiers in electromagnetics*, Ch. 1-3, Piscataway, NJ: IEEE Press, 2000.
- [12] C. Puente, J. Romcu, R. Pous, and A. Cardama, "On the behavior of the Sierpinski multiband antenna," *IEEE Trans. Antennas Propagat.*, vol. 46, pp. 517-524, Apr. 1998.
- [13] C. Puente and R. Pous, "Fractal design of multiband and low side-lobe arrays," *IEEE Trans. Antennas Propagat.*, vol. 44, pp. 730-739, May 1996.
- [14] J. Romeu and Y. Rahamat-Samii, "Fractal FSS: a novel dual-band frequency selective surface," *IEEE Trans. Antennas Propagat.*, vol. 48, pp. 1097-1105, Jul. 2000.
- [15] Y.-Q. Fu, N.-C. Yuan, and G.-H. Zhang, "A novel fractal microstrip pbg structure," *Microwave and Opt. Technol. Lett.*, vol. 32, pp. 136-138, Jan. 2002.
- [16] R. Borghi, F. Frezza, L. Pajewski, M. Santarsiero, and G. Schettini, "Full-wave analysis of the optimum triplicator," *J. of Electromagn. Waves and Appl.*, vol. 15, 689-707 (2001).
- [17] F. Frezza, L. Pajewski, and G. Schettini, "Characterization and design of two-dimensional electromagnetic band-gap structures by use of a full-wave method for diffraction gratings," to be published *IEEE Trans. Microwave Theory Tech.*.